Robust and Adaptive Lower Limb Prosthesis Stance Control via Extended Kalman Filter-Based Gait Phase Estimation

Nitish Thatte, Tanvi Shah, and Hartmut Geyer

Abstract—We present a control strategy for powered prostheses based on a robust estimate of the gait phase that is used to determine appropriate control actions. We use an extended Kalman filter (EKF) that fuses joint angle and velocity measurements to estimate the gait phase, which we define in this work to be a variable that progresses continuously during stance from zero at heel strike to one at toe-off. The control strategy uses the gait phase estimate as the input into Gaussian Process (GP) functions that specify the desired angles, velocities, and feedforward torques for the knee and ankle joints. We compare this proposed GP-EKF control strategy to two alternative controllers: A neuromuscular (NM) control strategy, which models leg muscles and hypothesized reflexes, and an impedance (IMP) control strategy. Our experiments involved seven able-bodied participants and a single amputee participant. We find that the GP-EKF control generated knee angle trajectories that were significantly closer to able-bodied walking data than those produced by either the NM or IMP controllers. However, ankle trajectories were less similar. In addition, we find in experiments with the participants stepping on blocks during stance that the GP-EKF control resulted in significantly fewer fall-like events than IMP control. Finally, we evaluate the ability of the proposed control to track the gait phase across both slowly and rapidly varying treadmill speeds and find that the EKF's phase estimate tracked these gait changes significantly better than a time-based phase estimate. The proposed control strategy may provide a robust and adaptive control alternative for powered prostheses.

Index Terms-Prosthetics and Exoskeletons, Sensor Fusion

I. Introduction

THE number of lower limb amputees in the United States is projected to increase from 1.6 million in 2005 to 3.6 million in 2050 [1]. Prosthetic legs currently prescribed to these lower limb amputees are mostly passive or semi-passive devices; unlike human limbs, they cannot produce positive net work over a gait cycle. Consequently, amputees often suffer from slow walking speeds, high energy consumption [2], and an increased risk of falling [3]. Development of active powered prostheses may help to address these gait deficiencies and improve the quality of life for amputees [4].

Manuscript received: Feb 23, 2019; Revised; May 5, 2019; Accepted: June 6.2019

This paper was recommended for publication by Editor Dr. Pietro Valdastri upon evaluation of the Associate Editor and Reviewers' comments. This work was supported by the National Science Foundation under Grant No. 1527140.

Nitish Thatte nitisht@cs.cmu.edu and Hartmut Geyer hgeyer@cs.cmu.edu are with the Robotics Institute and Tanvi Shah tjshah@andrew.cmu.edu is with Mechanical Engineering, Carnegie Mellon University, 5000 Forbes Avenue, Pittsburgh PA 15213, USA.

Digital Object Identifier (DOI): see top of this page.

Currently, the most widely used control method for powered transfemoral prostheses is finite state impedance control. This strategy divides the gait cycle into several discrete states, each with a different function mapping from joint angle and speed to torque [5]. This control method relies on the detection of gait events to trigger state transitions. Detection of these gait events is usually based on thresholds on sensor values, which as we show in section III, may be unreliable when gait is disturbed.

To achieve more robust control of lower limb prostheses, researchers have investigated alternative approaches. For example, neuromuscular controllers specify the desired behavior through models of muscle dynamics and hypothesized reflexes [6, 7]. However, a potential drawback of this approach is that neuromuscular models involve many parameters that may be difficult to tune, thus limiting clinical applicability.

Another alternative is control based on the continuous estimation of the phase of gait, usually defined as a number that increases monotonically from zero at heel strike to one at the next heel strike. For example, Holgate et al. [8] control an ankle prosthesis by using the polar angle between the tibia velocity and the tibia angle to estimate the phase of gait. This estimate, along with the stride length is then used to look up the desired ankle angle. Later work by Quintero et al. [9], found that for a transfemoral prosthesis, forming the polar plot with the integral of the hip angle instead of the velocity resulted in a more robust controller due to noise in the velocity signal during impacts. However, this approach was also found to be sensitive to stepto-step changes in gait due to drift in the hip angle integral term [10]. Rezazadeh et al. [10] eliminated the reliance on the hip integral by introducing discrete state transitions based on thigh angle and velocity thresholds. However, this approach may face similar robustness issues as the previously described finite-state impedance control.

Here we propose a control strategy for lower limb prostheses that avoids finite state transitions during stance and is able to quickly adapt to step-to-step gait variations. The control is built on a robust and smooth estimate of the phase of gait, which we define in this work as a variable that starts at zero at heelstrike and increases linearly to one at toe-off. In section II, we present an extended Kalman filter (EKF) that estimates the gait phase and its rate of change based on a multitude of sensor measurements. The control uses these estimates as inputs into Gaussian Process (GP) functions that specify the desired control actions for the prosthesis. In section III, we evaluate the performance of the proposed controller with experiments on able-bodied participants and a single amputee participant.

Finally, in section IV we discuss the results and highlight potential limitations of this study as well as avenues for future research.

II. Methods

The proposed prosthesis controller consists of two components. The first is an extended Kalman Filter (EKF) that estimates the gait phase, defined as the fraction of stance completed so far (section II-A). Ideally, the gait phase estimate starts at zero at heel strike and reaches one precisely at toe-off. The second component is a set of control surfaces, which are functions of gait phase and rate of change of phase (phase velocity), that provide desired knee and ankle angles, velocities, and feedforward torques for generating the prosthesis stance behavior (section II-B).

A. GP-EKF for estimating gait phase

In contrast to the previously described gait phase variable approaches for prosthesis control [8–10], which each use a single source of information, we take a sensor-fusion approach and combine angle and velocity information from the hip, knee, and ankle joints of the prosthetic limb. An IMU mounted to the thigh portion of CMU's powered knee-and-ankle prosthesis (fig. 2) provides information about the user's hip motion, and encoders on the prosthesis provide information about the knee and ankle joints. We use these observations in an extended Kalman filter (EKF) to estimate the gait phase and phase velocity during stance. The EKF assumes the linear, discrete time gait phase dynamics

$$x_t = \begin{bmatrix} \phi_t \\ \dot{\phi}_t \end{bmatrix} = \begin{bmatrix} 1 & \Delta t \\ 0 & 1 \end{bmatrix} \begin{bmatrix} \phi_{t-1} \\ \dot{\phi}_{t-1} \end{bmatrix} + w_t = Ax_{t-1} + w_t, \quad (1)$$

where ϕ is the gait phase, $\dot{\phi}$ is the rate of change of phase, Δt is the integration time step and $w_t \sim \mathcal{N}(0, Q)$. We set

$$Q = \begin{bmatrix} 0 & 0 \\ 0 & \sigma_{\dot{\phi}}^2 \end{bmatrix},\tag{2}$$

with $\sigma_{\dot{\phi}}^2=1\mathrm{e}{-7}$. These dynamics encode the assumption that the gait phase should evolve continuously, at a roughly constant rate.

Observations of the prosthesis-side hip, knee, and ankle angles and velocities inform the evolution of the above dynamics through learned Gaussian Process (GP) observation models. For the joint angles, the observation models are of the form

$$z_t^{\theta_j} = h^{\theta_j}(x_t) + v_t^{\theta_j} = GP_\mu^{\theta_j}(\phi_t) + v_t^{\theta_j}, \tag{3}$$

where $\mathrm{GP}_{\mu}^{\theta_j}$ is the mean of a learned GP model of the angle of joint j as a function of the gait phase ϕ and $v_t^{\theta_j} \sim \mathcal{N}\left(0,\mathrm{GP}_{\sigma^2}^{\theta_j}(\phi_t)\right)$. Here, $\mathrm{GP}_{\sigma^2}^{\theta_j}$ is the variance of the same learned GP model.

Similarly, for the joint velocities we use an observation model of the form

$$z_t^{d\theta_j/d\phi} = h^{d\theta_j/d\phi}(x_t) + v_t^{d\theta_j/d\phi} \dot{\phi}_t$$

$$= \left(GP_{\mu}^{d\theta_j/d\phi}(\phi_t) + v_t^{d\theta_j/d\phi} \right) \dot{\phi}_t$$
(4)

where $\mathrm{GP}_{\mu}^{d\theta_j/d\phi}$ is the mean of a Gaussian Process model of the velocity of joint j (in units of ${}^{d\theta_j/d\phi}$) as a function of ϕ . In addition, $v_t^{d\theta_j/d\phi} \sim \mathcal{N}\Big(0, \mathrm{GP}_{\sigma^2}^{d\theta_j/d\phi}(\phi_t)\Big)$, where $\mathrm{GP}_{\sigma^2}^{d\theta_j/d\phi}$ is the variance of the same learned GP model for joint velocity.

To train the GP observation models, the algorithm maintains a training data set of stance gait data. The training data set includes the joint angles and velocities (in units of $d\theta_j/d\phi$) sampled at 100 Hz as well as the actual corresponding gait phases and phase velocities during stance. We assume that, in hindsight, the actual gait phase increased linearly from zero at heel strike to one at toe-off and that the actual gait phase velocity was constant during stance and equal to $1/T_n$, where T_n is the duration of the completed stance. We retrain the GP models using this gait data after every five completed steps. To ensure that the test-time performance of the Gaussian Process models does not degrade as more training data accumulates, we employ the fully independent training conditional (FITC) approximation of the GP [11]. This approximation represents the GP using a fixed-size active set of training points. We use 25 points in our approximation.

With the learned GP observation models, we follow the GP-EKF procedure proposed by Ko and Fox [12] to obtain an estimate of gait phase and phase velocity. In this procedure, we first predict the next state distribution by propagating the mean $\hat{x}_{t-1|t-1}$ and covariance $\Sigma_{t-1|t-1}$ of the state using the dynamics model provided by eq. (1).

Next, we update the state distribution estimate using measurements z_t of the joint angles and velocities, the GP observation models,

$$h(x_t) = \begin{bmatrix} GP^{\theta}_{\mu}(\phi_t) \\ GP^{d\theta/d\phi}_{\mu}(\phi_t)\dot{\phi}_t, \end{bmatrix}$$
 (5)

and the optimal Kalman gain,

$$K_{t} = \sum_{t|t-1} H_{t}^{T} \left(H_{t} \sum_{t|t-1} H_{t}^{T} + M_{t} R M_{t}^{T} \right)^{-1}, \tag{6}$$

where,

$$H_{t} = \left. \frac{\partial h}{\partial x} \right|_{\hat{x}_{t|t-1}} = \begin{bmatrix} \frac{\partial GP_{\mu}^{\theta}/\partial \phi_{t}}{\partial \phi_{t}} \Big|_{\phi_{t}} & 0\\ \frac{\partial GP_{\mu}^{d\theta/d\phi}}{\partial \phi_{t}} \Big|_{\phi_{t}} \dot{\phi}_{t} & GP_{\mu}^{d\theta/d\phi}(\phi_{t}) \end{bmatrix}, \quad (7)$$

 $\hat{x}_{t|t-1}$ and $\Sigma_{t|t-1}$ are the propagated state and covariance respectively, $\mathrm{GP}_{\mu}^{\theta} = [\mathrm{GP}_{\mu}^{\theta_h}, \mathrm{GP}_{\mu}^{\theta_k}, \mathrm{GP}_{\mu}^{\theta_a}]^T$, and $\mathrm{GP}_{\mu}^{d\theta/d\phi}$, $\mathrm{GP}_{\sigma^2}^{\theta}$, and $\mathrm{GP}_{\sigma^2}^{d\theta/d\phi}$ are defined similarly,

$$M_t = \frac{\partial h}{\partial v_t} \bigg|_{\hat{x}_{t+1}} = \begin{bmatrix} I_{3\times3} & 0\\ 0 & \dot{\phi}_t I_{3\times3} \end{bmatrix}, \tag{8}$$

and

$$R_{t} = \text{blkdiag}\left(\text{GP}_{\sigma^{2}}^{\theta_{h}}(\phi_{t}), \text{GP}_{\sigma^{2}}^{\theta_{k}}(\phi_{t}), \text{GP}_{\sigma^{2}}^{\theta_{a}}(\phi_{t}), \text{GP}_{\sigma^{2}}^{\theta_{h}/d\phi}(\phi_{t}), \text{GP}_{\sigma^{2}}^{d\theta_{h}/d\phi}(\phi_{t}), \text{GP}_{\sigma^{2}}^{d\theta_{a}/d\phi}(\phi_{t})\right).$$
(9)

Due to the linearity of Gaussian processes and differentiation, we can analytically obtain derivatives required by eq. (7) using the methods provided by Solak et al. [13].

Finally, we reset the state distribution at heel strike to

$$\hat{x}_0 = \begin{bmatrix} 0 \\ 1/T_{n-1} \end{bmatrix}, \quad \Sigma_0 = 0_{2 \times 2}, \tag{10}$$

where T_{n-1} is the duration of the previous stance.

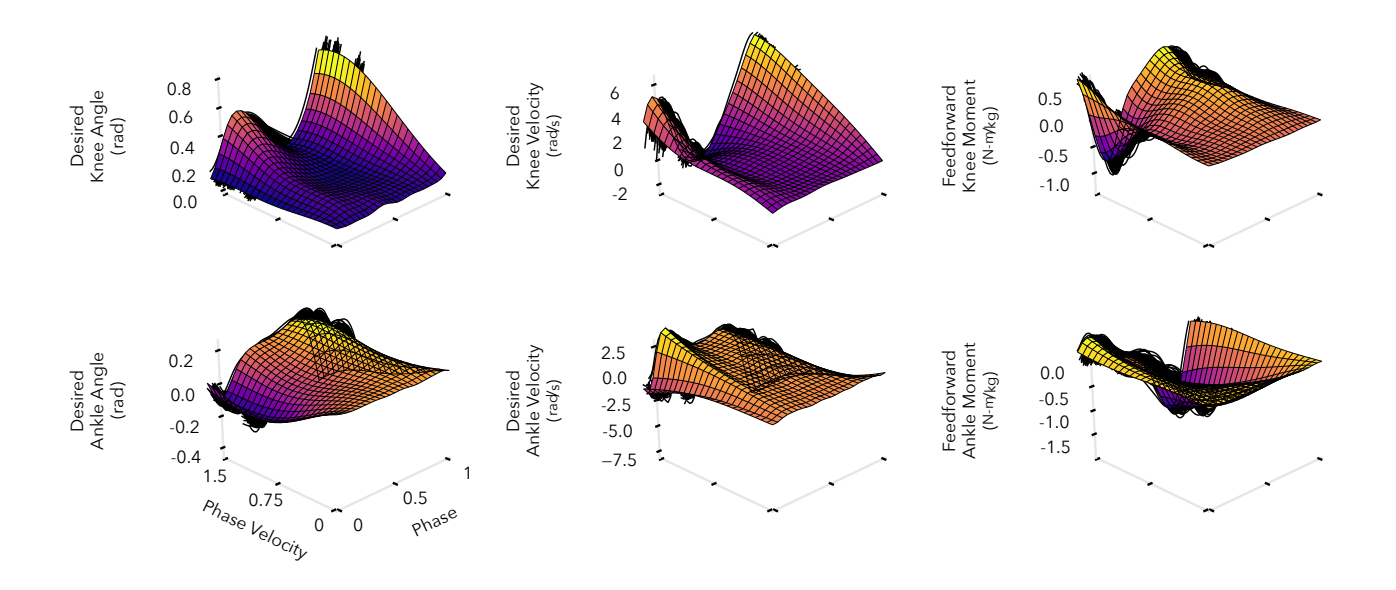


Fig. 1: Examples of learned control surfaces. We fit the surfaces to gait data from Moore et al. [14]. This data includes information for three speeds, 0.8, 1.2, and 1.6 m/s, which are shown as the clustered trajectories in the above panels. For an automatic transition to standing, the surfaces are additionally fit to virtual data that causes the joint angles to approach 5 deg, the velocities to approach 0 deg/s, and the joint torques to approach 0 N-m as the phase velocity goes to zero.

B. Control Surfaces

We use the mean estimates of the gait phase ϕ and phase velocity $\dot{\phi}$ as the inputs into learned control surfaces that provide the desired knee and ankle angles, velocities, and feedforward torques (Fig. 1). The final desired torques applied to the prosthesis are then given by

$$\tau_d = k_{\rm p} (\theta_{\rm d}(\phi, \dot{\phi}) - \theta) + k_{\rm d} (\dot{\theta}_{\rm d}(\phi, \dot{\phi}) - \dot{\theta}) + \tau_{\rm ff}(\phi, \dot{\phi}), \tag{11}$$

where $\theta_{\rm d}$, $\dot{\theta}_{\rm d}$, and $\tau_{\rm ff}$ are the learned control surfaces as functions of the estimated gait phase and phase velocity, $k_{\rm p}$ and $k_{\rm d}$ are proportional and derivative gains, and θ and $\dot{\theta}$ are the actual joint angle and velocity.

We learned nine sets of control surfaces by regressing the gait data of nine individual subjects. Each set of control surfaces is comprised of functions that map from the gait phase and phase velocity to desired knee and ankle angles, velocities, and feedforward torques. We obtain subject-specific gait data for nine subjects at three speeds, 0.8, 1.2 and 1.6 m/s, from the data set provided by Moore et al. [14]. For each subject in the data set, we split the gait data into individual stance portions and assumed that during each stance, the actual gait phase increased linearly from zero at heel strike to one at toe-off and the phase velocity during stance was constant and equal to 1/T, where T is the duration of stance. We again used sparse GP regression with the FITC approximation to regress the knee and ankle angles, velocities, and torques versus the gait phase and phase velocity. In this case, we used 100 active vectors to approximate each GP.

The gait data spans the whole range of gait phases ([0, 1]) but not the whole range of physiological phase velocities, as the gait speed only varies between 0.8 and 1.6 m/s. To ensure the

control surfaces generate smooth behaviors at slower speeds and when standing still $(\dot{\phi}=0)$, we additionally trained the GPs on a grid spanning $\phi \in [0,1]$ and $\dot{\phi} \in [0,\min(\dot{\phi}_{data~set})]$ with virtual training values derived by interpolating between the average trajectory at 0.8~m/s and desired values at $\dot{\phi}=0$. When $\dot{\phi}=0$, the desired joint angles, velocities and torques were set to 5 deg, 0~deg/s, and 0~N-m, respectively, thereby creating a smooth transition to a standing mode. Figure 1 shows examples of the resulting control surfaces derived from one subject's data.

C. Experimental Protocol

We evaluated the similarity of gait to able-bodied walking data and the robustness of our proposed controller in experiments conducted with seven able-bodied participants and an amputee participant. We additionally present data from an experienced user of the prosthesis (first author of paper), whose gait characteristics induced a different response from the prosthesis. All participants provided informed consent to IRB-approved protocols. The amputee participant wore the powered prosthesis prototype as shown in fig. 2a, while ablebodied participants used a shortened version of the prosthesis attached to an L-shaped adapter (fig. 2b). For more information on prosthesis specifications see chapter 3 of Thatte [15]. All participants had at least six hours of prior practice walking on the prosthesis. The able-bodied participants walked without assistance from handrails, while the amputee participant used the handrails for balance.

We compared our proposed control method to a stance control based on a neuromuscular model (NM) of human neurophysiology [16] and to finite state impedance control

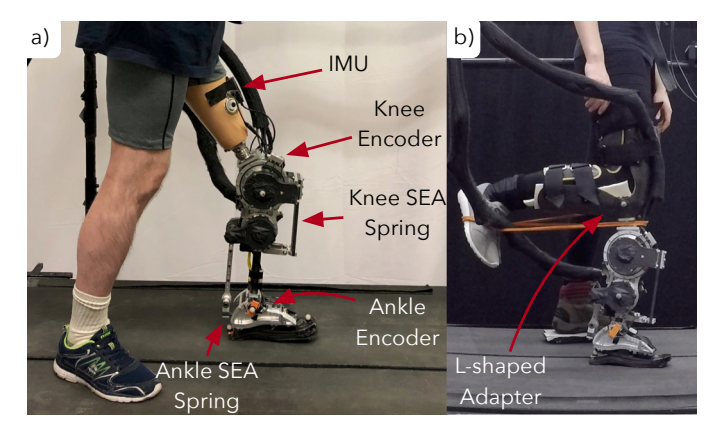


Fig. 2: CMU powered prosthesis used in experiments. a) Prosthesis configuration for amputee testing. b) Prosthesis configuration for able-bodied testing with L-shaped adaptor.

(IMP) [17]. For these controllers, we generated parameter sets by fitting control parameters to the same nine subjects' gait data used to generate the control surfaces described in section II-B. For the IMP control, we used a threshold on the knee angle to specify the transition between the first and second stance states and a threshold on the ankle angle to specify the transition between the second and third stance states. For specifics on methods for finding parameters for these two control strategies, see Thatte [15] section 7.2.1. Prior to beginning the experiments, participants walked with each of the nine control surfaces for the GP-EKF control and each of the nine parameter sets for the NM and IMP controllers and indicated their preferred setting for each controller type. All three stance control strategies were paired with the same swing control strategy, in which minimum jerk trajectories for the knee and ankle are generated at toe-off and tracked with PD-feedback combined with a model-based feedforward term as in Lenzi et al. [18]. In total, we conducted four experiments:

- (1) A test of the ability of each control strategy to produce a normal walking gait pattern. Able-bodied participants walked without the use of handrails at 0.8 m/s and the amputee participant used the handrails and walked at 0.6 m/s. All participants walked with their preferred parameters for each controller for one minute. We compared the resulting prosthesis knee and ankle kinematics and kinetics to able-bodied gait data [19]. The amputee subject only participated in this portion of the experiment.
- (2) A comparison of the robustness of the three controllers to ground height disturbances. We simulated a ground disturbance by having participants step on 3 cm blocks placed on the treadmill. We tested the controllers in a random order in an ABCCBA sequence. In each trial, the participants stepped on blocks 20 times. We recorded the number of fall-like events (FLEs), defined as instances when participant needed support from either the handrails or a ceiling mounted harness to regain balance.
- (3) A test of the adaptability of the gait phase estimate. To test the adaptability, we had participants use the proposed GP-EKF control while the treadmill speed varied sinusoidally between 0.4 and $1.2\,\mathrm{m/s}$ with a 20 s period. We compared the

gait phase and phase velocity estimates given by the EKF filter to the true gait phase, assumed to increase linearly from zero at heel strike to one at toe-off, and the true phase velocity, assumed to equal $1/T_n$, where T_n is the duration of the current stance. As a baseline, we compared the EKF to time-based gait phase and phase velocity estimates, which assume the duration of the current stance will be the same as the previous stance, resulting in the gait phase and phase velocity estimates

$$\phi_{\text{time based}} = t_n / T_{n-1} \tag{12}$$

$$\dot{\phi}_{\text{time based}} = 1/T_{n-1},\tag{13}$$

where t_n is the time after heel-strike of the current stance and T_{n-1} is the duration of the last stance.

(4) Finally, a test of the ability of the GP-EKF control to respond to sudden treadmill stops. If the participant stops his or her gait, then the gait phase estimate should stabilize and the phase velocity should trend towards zero. The corresponding desired joint angles should approach 5 deg as shown in fig. 1.

We assess significant differences between conditions via the two-sided paired Wilcoxon signed rank test [20]. Experienced participant data was not considered for significance testing.

III. RESULTS

A. Comparison to Able-Bodied Gait Kinematics and Kinetics

Figure 3 shows the average knee and ankle angles as well as the corresponding joint moments generated by the prosthesis controllers during undisturbed walking at 0.8 m/s. All three control strategies produce knee angle trajectories that are similar to the able-bodied data (first row). The neuromuscular (NM) control, however, seems to suffer more from knee overextension during mid-stance and less knee flexion at the end of stance. For some able-bodied subjects, and to a substantial degree for the amputee subject, the knee overextension causes the joint to engage the mechanical hard-stop on the prosthesis. This triggers a sudden rise in knee torque. Figure 4a summarizes the root-mean-squared (RMS) error between the mean ablebodied knee kinematics and the median knee kinematics of each subject. The GP-EKF control strategy produced knee trajectories that are significantly more kinematically similar to able-bodied walking data than those produced by IMP or NM control.

The second row of fig. 3 shows the average ankle trajectories for each control strategy. In this case, the GP-EKF control produced trajectories that were the least similar to ablebodied data. As shown in fig. 4b, this trend reached statistical significance compared to impedance (IMP) control, which produced trajectories most similar to able-bodied walking data. The dissimilarity of the GP-EKF controller's ankle trajectories to the able-bodied reference is largely due to (1) a lack of ankle push-off plantar flexion in late stance and (2) a lack of dorsiflexion during mid-stance for 3 out of 8 subjects, who all chose the same control surface set.

Finally, the third and fourth rows of fig. 3 show the knee and ankle moments for the three controllers. IMP control produced knee moments most like those seen in able-bodied walking by a significant margin (fig. 4c), whereas the GP-EKF and NM controllers performed comparably. Although the GP-EKF

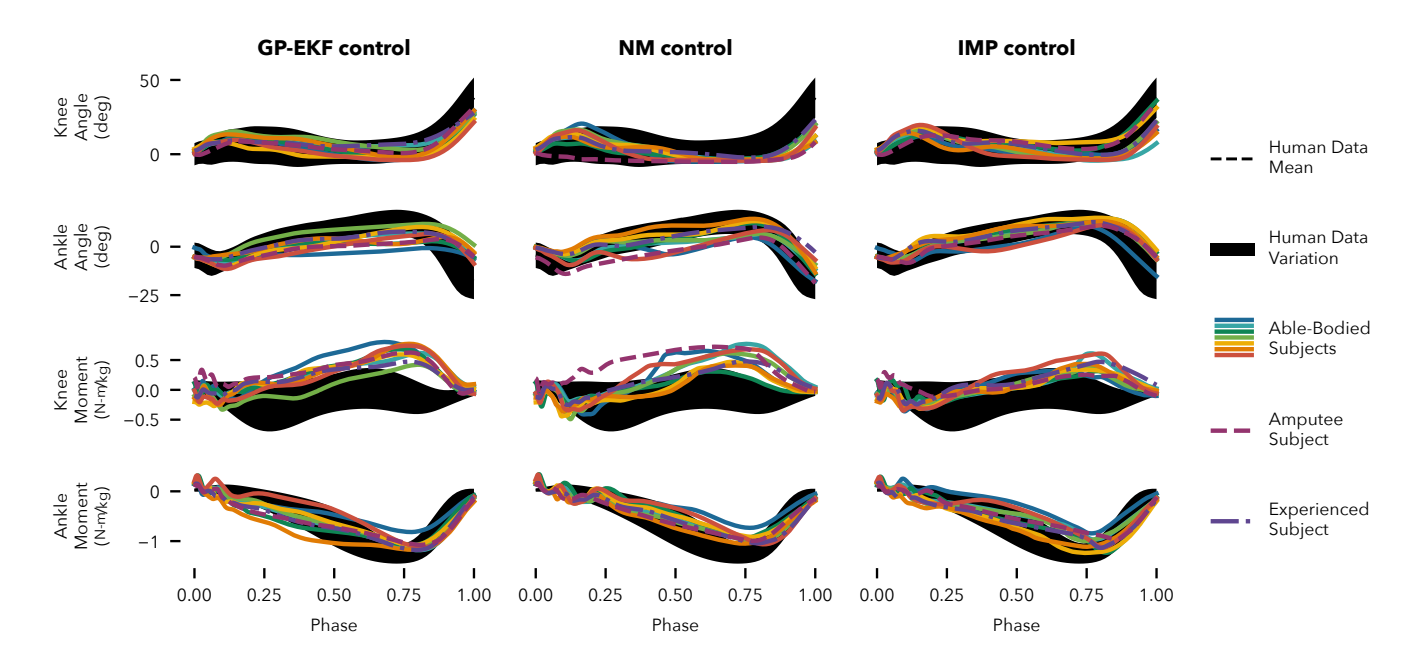


Fig. 3: Comparison to able-bodied gait kinematics and kinetics. Average knee angle (row 1), ankle angle (row 2), knee moment (row 3), and ankle moment (row 4) for the GP-EKF controller (column 1), neuromuscular controller (column 2), and impedance controller (column 3). Black dashed lines and gray shaded areas show the mean and two standard deviations for very slow human walking data (from [19]).

control's ankle moments were the least similar to the ablebodied ankle moments, the absolute differences were small (fig. 4d).

B. Robustness to Ground Height Disturbances

Figure 5 shows the number of times able-bodied subjects fell with each control strategy when stepping on blocks. Subjects fell significantly more often with the IMP control compared to either the GP-EKF or NM controllers. However, when using the neuromuscular control the experienced user fell 8 times, more than any other subject in any condition.

C. Adaptability of Gait Phase Estimate

The adaptability of the gait phase estimate was tested by sinusoidally varying the treadmill speed during walking. Figure 6 shows the average RMS errors of the EKF-based gait phase estimate and time-based phase estimate compared to the ground-truth phase obtained in hindsight. For all subjects, the EKF tracked the true phase significantly more accurately than did the time-based phase estimate.

For a more specific example, fig. 7 shows the gait phase estimates during the treadmill speed variation experiment for a single subject. Because the initial conditions of the EKF and the time-based phase estimates are identical (compare eq. (10) and eq. (13)), the phase estimates are similar in early stance. As the treadmill speed changes from one step to the next, the time-based phase estimate diverges significantly from the true phase. The EKF, on the other hand, is able to recover to the true phase towards the end of stance and more accurately predicts the toe-off event.

D. Response to Sudden Treadmill Stops

Finally, fig. 8 shows the gait phase (a), and phase velocity (b) estimates when the treadmill is suddenly stopped halfway through the stance phase. The EKF's phase estimates (solid lines) reflect the fact that the gait cycle has halted, as they do not continue to progress to one. Moreover, when the treadmill stops, the knee (c) and ankle angles (d) approach 5 deg as desired for standing (compare fig. 1). In contrast, the time-based phase estimates (dashed lines in panels (a) and (b)) continue at their initial rate, with the phase reaching one.

IV. Discussion

We proposed a new approach for the control of powered transfemoral prostheses. The approach uses a robust estimate of the gait phase derived from an EKF that integrates multiple sensor measurements to determine the desired knee and ankle angles, velocities, and torques from trained control surfaces. The proposed approach produced knee kinematics that were more similar to able-bodied walking data than did NM or IMP control, matched NM control and improved upon IMP control in terms of gait robustness to ground height disturbances, and adapted the phase estimate to both gradual and abrupt changes in speed more quickly than a time-based phase estimate.

We believe that a key reason for the robustness improvements of the proposed GP-EKF control and NM control over IMP control is the smoothness of the gait phase estimation in these two controllers. In NM control, the gait phase estimation is implicit and encoded in the internal states of virtual muscles, which are modulated by musculoskeletal dynamics and reflexes. In the proposed control presented here, the EKF directly infers a robust estimate of the gait phase from multiple measurements.

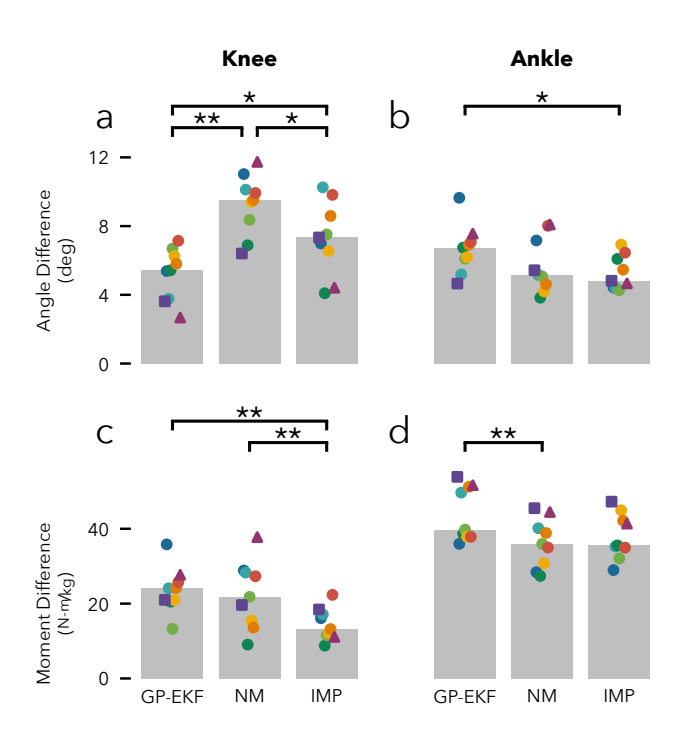


Fig. 4: Average difference between prosthetic and able-bodied walking kinematics (a,b) and kinetics (c,d) produced by the three different controllers. GP-EKF resulted in significantly smaller differences in knee angles than NM or IMP control, but slightly greater differences in ankle angles and joint torques. Grey bars show median of subject data, circle markers indicate able-bodied subject data, triangle markers indicate amputee data, and square markers indicate experienced able-bodied user data. *: p < 0.05, **: p < 0.01.

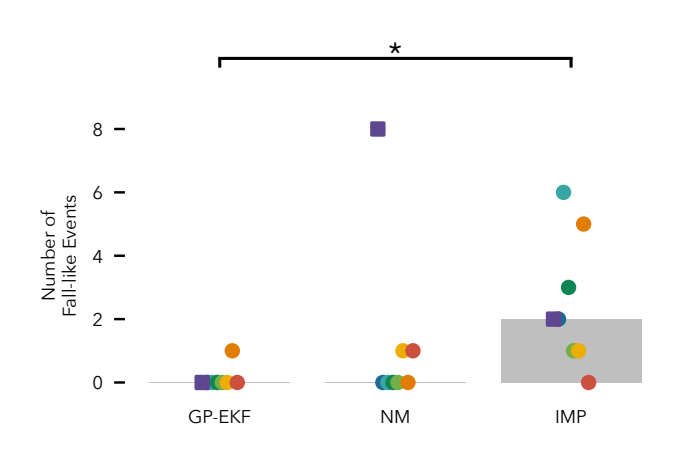


Fig. 5: Robustness to ground height disturbances. Number of fall-like events (FLEs) accrued for each controller during ground height disturbance trials. GP-EKF control significantly reduced the number of FLEs compared to IMP control. Grey bars show median of subject data, circle markers indicate ablebodied subject data, and square markers indicate experienced able-bodied user data. *: p < 0.05.

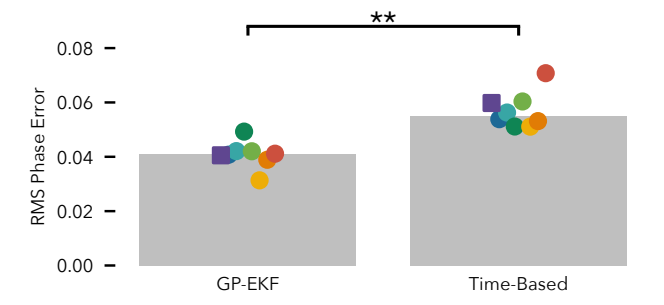


Fig. 6: Adaptability of gait phase estimate. Mean phase error of EKF versus time-based phase estimation when walking with sinusoidally varying treadmill speed. The EKF significantly improves phase tracking compared to the time-based estimate. Grey bars show medians of subject data, circle markers indicate able-bodied subject data, and square markers indicate experienced able-bodied user data. **: p < 0.01.

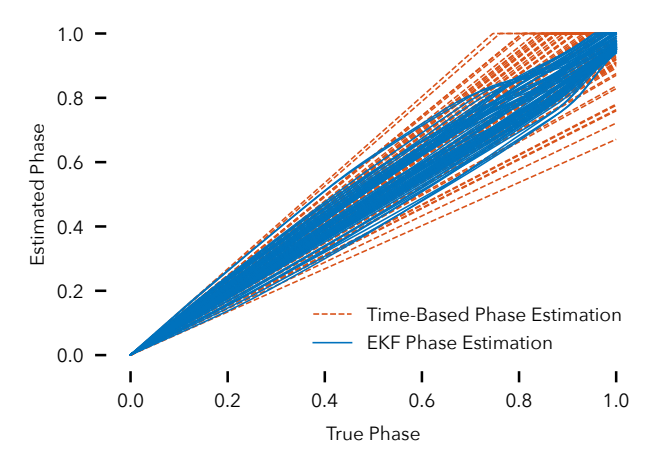


Fig. 7: Example of EKF-based gait phase estimation (red) versus time-based phase estimation (blue) for one subject. Due to step-to-step speed variations caused by the sinusoidally varying treadmill speed, the time-based phase estimation accrues significant errors. In contrast, the EKF-based phase estimate is able to respond to changes in gait within the gait cycle, thus reducing phase estimation errors.

In either case, the resulting control commands are smooth and do not normally change abruptly from one moment to the next. In contrast, IMP control estimates a discrete notion of the gait phase by splitting the stance portion of gait into three states that are triggered by joint angle thresholds. Consequently, in the ground height disturbance experiments, subjects were occasionally caught off-guard by unexpected transitions, triggered by abnormal kinematics when stepping on a block, which then caused large, sudden changes in torque. Unexpected state transitions between the mid-stance and late-stance state were especially consequential, as in the late-stance state, knee torque trends towards zero to allow for passive knee flexion, while the ankle plantarflexes. If a user's center of mass is positioned incorrectly, this combination of joint torques can

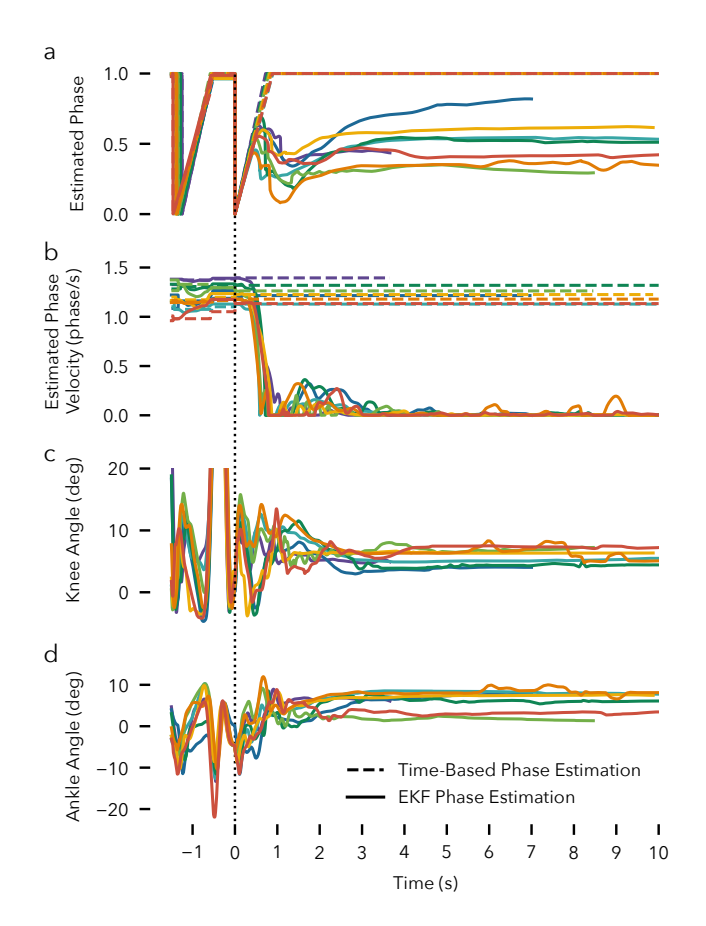


Fig. 8: Response to sudden treadmill stops. Estimated gait phase (a) and phase velocity (b), and the measured knee (c) and ankle (d) angles when the treadmill is suddenly stopped halfway through stance. When gait stops, the EKF-estimated phase stabilizes to a constant value (solid traces), phase velocity falls to zero, and the joint angles approach 5 deg as desired by the control surfaces (compare fig. 1). The time-based phase estimate fails to respond (dashed lines). Vertical black dotted line indicates heel strike of final stance.

cause a sudden collapse of the knee, which was the cause for many of the observed FLEs with IMP control.

NM control too can result in unexpected FLEs due to incorrect gait phase estimation. The experienced user fell a total of eight times when stepping on blocks with the NM control (see square marker fig. 5). These FLEs were the result of a modeled reflex that reduces knee extensor muscle stimulation in late stance in proportion to ankle plantarflexion, thereby allowing for passive knee flexion leading into swing. In contrast to less experienced subjects, the experienced user was able to control the knee over-extension during stance and achieve more normal knee flexion in late-stance during normal walking (see fig. 3 row 1, column 2), However, this increased knee flexion during normal walking may have increased the prosthesis' susceptibility to premature knee collapse when disturbed. While the modeled neuromuscular reflexes seem to work well during steady-state walking and during disturbed walking for inexperienced users, the large increase in FLEs

for the experienced user exposes the difficulty of relying on heuristic reflexes to obtain robust control across a range of gait characteristics. In contrast, the proposed EKF approach takes a principled approach to gait phase estimation and thus resulted in the fewest FLEs.

Some improvements can be made in the implementation of the proposed control. First, the normal walking experiments revealed that the ankle trajectories produced by the GP-EKF control were significantly less similar to able-walking data than those produced by NM or IMP controls (see fig. 4b). The GP-EKF ankle trajectories in fig. 3 show that peak ankle flexion is achieved later in stance and that the ankle insufficiently plantarflexes at toe-off. These kinematic issues are also present in the desired angles commanded by the GP control surfaces. Therefore, this issue likely stems from a premature cutoff between stance and swing in the gait dataset used to generate the control surfaces. Extending the training data stance duration slightly should increase the desired ankle plantarflexion at the end of stance and engage the peak ankle dorsiflexion earlier. Improving the ankle's push off through this change may also help increase the comfortable walking speed achievable with this control strategy from 0.8 m/s for the able-bodied subjects and 0.6 m/s for the amputee-subject to closer to a typical walking speed for an able-bodied adult of 1.2 m/s [19].

Second, in the current study, we held constant the impedance about the desired trajectory, represented by k_p and k_d in eq. (11). However, recent research has investigated how impedance varies continuously throughout gait [21]. These results could be used to parameterize impedance as a function of gait phase. Taking this step could help improve the similarity of the knee and ankle torques produced by the GP-EKF controller to those seen in able-bodied walking data. However it is important to note, the closeness of prosthetic gait to able-bodied walking data may not be the best metric of prosthesis performance, as amputee requirements may be significantly different from non-amputees. Therefore, further research should also focus on determining improved performance metrics for powered prostheses.

Our work bears some resemblance to the complementary limb motion estimation (CLME) approach proposed by Vallery et al. [22]. This approach uses linear regression to learn a direct mapping between the angles and velocities of the user's limbs to the prosthesis' joint angles and velocities. There are two key differences between our and the CLME approach. First, our approach only uses signals from sensors mounted to the prosthesis itself, whereas the CLME approach used many IMUs mounted to the torso and sound side leg. Donning these sensors may be impractical for everyday use by an amputee in the real world. Second, the CLME approach directly maps from human to prosthetic joint angles and velocities via linear regression. In contrast, our approach goes through the latent gait phase and phase velocity states first, which decouples the observation models from the prosthesis control models. This allows us to separately learn the observation models and tune the control models to optimize user preference and performance.

There are several avenues for future research to expand the proposed control approach. First, we only used prosthesis joint angles and velocities for the observation models. It is worth investigating if additional measurements such as ground reaction forces, accelerations, and EMG signals improve the state estimate. Second, we used a simple, two-state model to represent the entirety of the coupled human-prosthesis state during stance. Adding additional state variables may help capture important behaviors such as balance recovery actions taken by the upper body. To this end, dimensionality reduction techniques could help identify better state representations from gait data. New state representations need to satisfy two constraints that our current model satisfies: (1) The evolution of the state needs to approximately abide by some Markov dynamics model so we can perform the predict step of the EKF. (2) The evolution of state throughout stance should be knowable in hindsight after a step is completed so that the observation model can be learned online. Fourth, with more advanced state and observation models, more advanced forms of state estimation may be necessary, including unscented Kalman filters or particle filters such as the one proposed by Dhir et al. [23], which allows for continuous gait phase estimation using discrete heel and toe contact sensors. Finally, in this work, we focused on phase estimation and control of the stance portion of the gait cycle. However, in future work we could instead define the gait phase as starting at zero at heel strike and progressing to one at the next heel strike, thereby allowing the phase estimate to parameterize both the stance and swing behaviors.

V. Conclusion

In this work, we have demonstrated a novel prosthesis controller based on a robust and smooth estimate of the phase of gait derived from an EKF. Crucially, the proposed GP-EKF control was more robust to ground height disturbances than the popular finite-state impedance control strategy and was able to adapt to gait changes within a single gait cycle. While we can likely make further improvements to the control strategy, the work highlights the importance of reliable state estimation for robust prosthesis control.

ACKNOWLEDGMENT

The authors would like to thank Professor Goeran Fiedler of the University of Pittsburgh for amputee subject recruitment and help running experiments and Timothy Kyung for his help conducting experiments as well.

REFERENCES

- K. Ziegler-Graham, E. J. MacKenzie, P. L. Ephraim, T. G. Travison, and R. Brookmeyer, "Estimating the prevalence of limb loss in the united states: 2005 to 2050," *Archives of physical medicine and rehabilitation*, vol. 89, no. 3, pp. 422–429, 2008.
- [2] R. Waters, J. Perry, D. Antonelli, and H. Hislop, "Energy cost of walking of amputees: the influence of level of amputation," *J Bone Joint Surg Am*, vol. 58, no. 1, pp. 42–46, 1976.
- [3] W. C. Miller, M. Speechley, and B. Deathe, "The prevalence and risk factors of falling and fear of falling among lower extremity amputees," *Archives of physical medicine and rehabilitation*, vol. 82, no. 8, pp. 1031–1037, 2001.

- [4] M. Windrich, M. Grimmer, O. Christ, S. Rinderknecht, and P. Beckerle, "Active lower limb prosthetics: a systematic review of design issues and solutions," *Biomedical engineering online*, vol. 15, no. 3, p. 140, 2016.
- [5] F. Sup, H. A. Varol, J. Mitchell, T. J. Withrow, and M. Goldfarb, "Preliminary evaluations of a self-contained anthropomorphic transfemoral prosthesis," *IEEE/ASME Transactions on mechatronics*, vol. 14, no. 6, pp. 667–676, 2009.
- [6] M. F. Eilenberg, H. Geyer, and H. Herr, "Control of a powered ankle-foot prosthesis based on a neuromuscular model," *IEEE transactions on neural systems and rehabilitation engineering*, vol. 18, no. 2, pp. 164–173, 2010.
- [7] N. Thatte and H. Geyer, "Toward balance recovery with leg prostheses using neuromuscular model control," *IEEE Transactions on Biomedical Engineering*, vol. 63, no. 5, pp. 904–913, 2016.
- [8] M. A. Holgate, T. G. Sugar, and A. W. Bohler, "A novel control algorithm for wearable robotics using phase plane invariants," in 2009 IEEE International Conference on Robotics and Automation. IEEE, 2009, pp. 3845–3850.
- [9] D. Quintero, D. J. Villarreal, and R. D. Gregg, "Preliminary experiments with a unified controller for a powered knee-ankle prosthetic leg across walking speeds," in 2016 IEEE/RSJ International Conference on Intelligent Robots and Systems (IROS). IEEE, 2016, pp. 5427–5433.
- [10] S. Rezazadeh, D. Quintero, N. Divekar, and R. D. Gregg, "A phase variable approach to volitional control of powered knee-ankle prostheses," in 2018 IEEE/RSJ International Conference on Intelligent Robots and Systems (IROS). IEEE, 2018, pp. 2292–2298.
- [11] E. Snelson and Z. Ghahramani, "Local and global sparse gaussian process approximations," in *Artificial Intelligence and Statistics*, 2007, pp. 524– 531.
- [12] J. Ko and D. Fox, "GP-BayesFilters: Bayesian filtering using gaussian process prediction and observation models," *Autonomous Robots*, vol. 27, no. 1, pp. 75–90, 2009.
- [13] E. Solak, R. Murray-Smith, W. E. Leithead, D. J. Leith, and C. E. Rasmussen, "Derivative observations in gaussian process models of dynamic systems," in *Advances in neural information processing systems*, 2003, pp. 1057–1064.
- [14] J. K. Moore, S. K. Hnat, and A. J. van den Bogert, "An elaborate data set on human gait and the effect of mechanical perturbations," *PeerJ*, vol. 3, p. e918, 2015.
- [15] N. Thatte, "Design and evaluation of robust control methods for robotic transfemoral prostheses," Ph.D. dissertation, Carnegie Mellon University, May 2019.
- [16] N. Thatte, H. Duan, and H. Geyer, "A method for online optimization of lower limb assistive devices with high dimensional parameter spaces," in 2018 IEEE International Conference on Robotics and Automation (ICRA). IEEE, 2018, pp. 1–6.
- [17] B. E. Lawson, J. Mitchell, D. Truex, A. Shultz, E. Ledoux, and M. Gold-farb, "A robotic leg prosthesis: Design, control, and implementation," *IEEE Robotics & Automation Magazine*, vol. 21, no. 4, pp. 70–81, 2014.
- [18] T. Lenzi, L. Hargrove, and J. Sensinger, "Speed-adaptation mechanism: Robotic prostheses can actively regulate joint torque," *IEEE Robotics & Automation Magazine*, vol. 21, no. 4, pp. 94–107, 2014.
- [19] G. Bovi, M. Rabuffetti, P. Mazzoleni, and M. Ferrarin, "A multiple-task gait analysis approach: kinematic, kinetic and emg reference data for healthy young and adult subjects," *Gait & posture*, vol. 33, no. 1, pp. 6–13, 2011.
- [20] J. D. Gibbons and S. Chakraborti, "Nonparametric statistical inference," in *International encyclopedia of statistical science*. Springer, 2011, pp. 977–979.
- [21] H. Lee, E. J. Rouse, and H. I. Krebs, "Summary of human ankle mechanical impedance during walking," *IEEE journal of translational* engineering in health and medicine, vol. 4, pp. 1–7, 2016.
- [22] H. Vallery, R. Burgkart, C. Hartmann, J. Mitternacht, R. Riener, and M. Buss, "Complementary limb motion estimation for the control of active knee prostheses," *Biomedizinische Technik/Biomedical Engineering*, vol. 56, no. 1, pp. 45–51, 2011.
- [23] N. Dhir, H. Dallali, E. M. Ficanha, G. A. Ribeiro, and M. Rastgaar, "Locomotion envelopes for adaptive control of powered ankle prostheses," in 2018 IEEE International Conference on Robotics and Automation (ICRA). IEEE, 2018, pp. 1488–1495.